IOP Conf. Series: Materials Science and Engineering **115** (2016) 012001 doi:10.1088/1757-899X/115/1/012001

Cellular Automata Modeling of Decarburization of Metal Droplets in Basic Oxygen Steelmaking

Ankit[1], T. K. Kundu

Department of Metallurgical and Materials Engineering, Indian Institute of Technology Kharagpur, Kharagpur, West Bengal--721302, India

[1]E-mail: ankitv89@gmail.com

Abstract. In steelmaking, a supersonic jet is blown over the bath to refine the hot metal to produce steel. The refining process primarily consists of removal of impurities from the hot metal to a permissible level. The impact of oxygen jet on the surface of the hot metal bath results in ejection of droplets, which mix with slag and form emulsion. The formed emulsion plays an important role in refining reactions kinetics and understanding of this process is required todevelopimproved process control model for the steel industry. In this paper, cellular automata technique has been explored to simulate decarburization in emulsion caused by interfacial reactions between the metal droplets and slag. In the course of the work, a framework has also been developed to quantify the contribution of carbon monoxide, generated by decarburization, in bloating of metal droplets and formation of halo around the droplets. The model has incorporated diffusion and decarburization reaction based on probabilities to study the evolution of the system. Simulations with varying parameters have been performed and decarburization trends obtained are comparable with the experimentally determined data reported in literatures.

Keywords: Steelmaking, Decarburization, Cellular Automata, Kinetics

1. Introduction

The blast furnace - basic oxygen furnace (BF-BOF) is the most dominant routes for steel production due to high productivity and efficiency of the process [1]. In BOF steelmaking, the hot metal from the blast furnace is poured into a specially designed converter along with scrap and flux. The input hot metal is in the temperature range of 1300 - 1400^{o}C and contains carbon, silicon, phosphorous and other impurities. The objective of the steel making process is to refine the hot metal by removing these impurities to a predefined target level by oxidising these impurities and then separating their oxides from the hot metal. The Carbon is removed in gaseous form whereas remaining impurity oxides are removed as slag. The oxidizing atmosphere is achieved by blowing a jet of supersonic oxygen over the metal bath surface as depicted schematically in Fig. 1. The amount of flux (CaO and MgO) is decided by the amount of impurities in the hot metal, mainly silicon and phosphorous. The scrap is added to utilize the excess heat generated by oxidation of impurity species. With time, the CaO dissolves and mixes with silica (formed by oxidation of silicon) and forms the slag. Slag mainly consists of SiO_2, CaO and FeO, and the important parameters for the refining process are basicity and oxidation potential of the slag. Also, upon impact of oxygen jet, metal droplets are ejected from the metal surface into the slag resulting in formation of emulsion. There have been varying estimates of the extent of reactions occurring in the emulsion, varying from insignificant to as high

as 78% [2, 3]. Recent studies have highlighted the importance of reaction in emulsions and deeper understanding of the phenomenon occurring in the emulsion [4-8]. Mainly two phenomena have been observed when the metal droplets undergo reactions in emulsion; a) formation of halo around the droplet [9] and b) bloating or swelling of the droplet [10]. The exact conditions for occurrence of either or both of these phenomena are still a matter of further study. Mulholland et. al. [9] have carried out a detailed study of decarburization using X-ray fluoroscopy technique. They have observed formation of halo around the droplet, however, Sarkar [11] has expressed some uncertainties about whether the droplets nucleated inside the droplet or at the interface. Similarly, Molleseau and Fruehan [10] have studied the decarburization in the droplet and observed bloating of droplet. Brooks et. al. [12] have highlighted the role of bloating on the residence time of the droplet which in turn affects the decarburization kinetics of the bath. They have also developed a bloating model known as 'Bloated Droplet Theory' to estimate the degree of bloating of a droplet based on the decarburization rate [12]. The bloating of droplet increases the residence time of the droplet in the emulsion which affects the extent of reactions occurring in emulsion phase. However, conditions under which either of these two mechanisms will dominate is still not clear. To resolve the issue of selection of mechanism, Chen and Coley [13] have conducted a series of experiments. They have highlighted the role of oxygen potential and carbon concentration on the selection of mechanism. They also have highlighted the role of nucleation and growth of carbon monoxide bubbles in occurrence of bloating [14]. They have concluded that classical nucleation theory can explain the nucleation and growth of droplet but the value of interfacial surface tension values has to be around 40 times lower than that of its theoretical value. Kinetics studies have also been performed by Gaye and Riboud [15] using droplets and slag of different chemical composition and oxidizing power. In continuation, Wei Pan et. al, [16] have conducted similar experiments with different mass and have considered the effect of stirring also. Both of them have concluded that decarburization characteristics depends on the initial carbon content as well as oxidizing power of the slag. For modeling of decarburization, some empirical models as well as mathematical models have been proposed, however, only the model developed by Dogan et. al. [4-6] have distinguished between the decarburization occurring in emulsion and metal bath. Using bloated droplet theory they have estimated the residence time of the droplets in the slag and calculated the total decarburization in the emulsion was based on it. Sun [17] has derived and solved a set of partial differential equations to analyse the behaviour of species inside the droplet. The model is not limited to decarburization and have also analysed desiliconization and composition distribution of generated carbon monoxide.

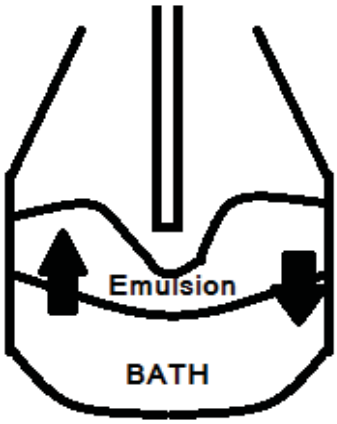

Figure 1. Schematic of a LD converter

These work clearly show that the behavior of metal droplets in emulsion is a very complex and it is difficult to model using traditional deterministic approach. So, use of cellular automata (CA) is proposed to develop

a simulation method of decarburization reaction occurring in the emulsion. The ability of cellular automata to generate complex patterns using simple local rules makes it a very powerful technique for modeling physical and biological systems. The CA came in light by works of Von Neumann who was working on self-replicating biological systems [18]. Based on advice by Ulman, Von Neumann developed a two dimensional CA with 29 states capable of self-generating [19]. In subsequent decades, CA has been applied to urban planning [20], medical research [21, 22] and financial modelling [23, 24], thus, demonstrating its vast application base. In metallurgical context, CA has been extensively used to study recrystallization in steels but its application to reactions occurring during steelmaking operation is still unexplored as far as authors' knowledge. With regard to study of general chemical systems, Seybold and group [25] have demonstrated the use of stochastic approach with CA to simulate first order reactions including decay, opposing, sequential and irreversible reactions. Their work has highlighted the use of simple CA rules with a probability factor to simulate first order reactions. Further works have utilized the methodology to simulate acid dissociation [26]. Neuforth and co-workers [27] have used the CA to model kinetically and thermodynamically controlled processes. The work of Neuforth is then extended to model CSTR reactors [28]. On the front of diffusion reactions, Chopard and Droz [29], Weimar [30] and Adamatzky et. al. [31] have demonstrated the use of CA. A recent work by Ween et. al. [32] has attempted to describe the reaction between $CaCO_3$ and HCl using CA. They also have developed a PDE based model and validated it with experimental data. The authors also have noted that CA model can be related to physical time either exponentially or linearly.

In our present work, we have explored cellular automata approach to simulate decarburization in metal droplets under steelmaking conditions. The model is tested under different oxygen and carbon concentrations and an effort is also made to investigate situations that may cause halo and bloating of the droplet.

2. Theory of Cellular Automata

A cellular automata system is described by a i) lattice cells, ii) state of cells, iii) neighbourhood function and iv) transition function [33].The lattice can be visualized as a set of cells which form a grid. All transitions steps are operated upon these cells and the lattice provides platform for those transitions. Each of those cells has a state which defines its identity. The cells have a neighbourhood i.e. a methodology for selection of particles to form its neighbourhood. The neighbourhood commonly used are Newman's neighbourhood as shown in Fig. 2 or Moore's neighbourhood as shown in Fig. 3. The transition functions update the state of the cell. The transition function uses a rule table, which is based on the neighbourhood of the cell, to decide upon the appropriate transition. For example, one of the rules in the rule table can state that if a cell in the lattice with state 1 is surrounded by cells in Newmann's neighbourhood with state 0, then the state of the concerned cell should be changed to 0 from 1. The transition function, evaluates the cell for neighbourhood and if the condition is satisfied, the cell's state is updated from 1 to 0. The rules are generally simple and are designed based on the system under consideration.

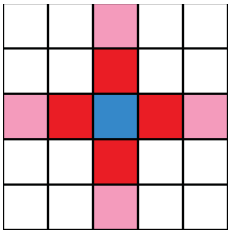

Figure 2. Newmann Neighbourhood

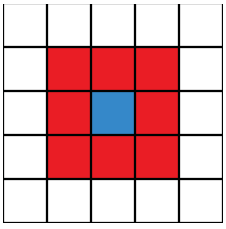

Figure 3. Moore's Neighbourhood

3. Model Development

In steelmaking, the overall reaction in slag phase can be divided into the following steps: a) migration of FeO from slag to the reaction interface, b) dissociation of FeO into Fe and O and c) reaction of O with carbon at the interface and lastly d) removal of the products. Similarly, reaction steps involved in metal phase are: a) migration of carbon from metal towards the reaction interface, b) oxygen diffusion through the interface into the metal droplet, c) reaction of carbon and oxygen and d) removal of products [16]. Sun [17] has simulated the concentration profile in the metal droplet and assumed that the rate controlling steps is the migration of FeO towards the slag interface and diffusion of species inside the metal droplet. The reaction at the interface can be assumed to be fast. Also, the formation of gas halo will add an additional barrier for migration of species to and from the reaction interface. However, in the present model, migration through gas halo is not considered. The objective here is to simulate the situations inside the droplets which may lead to either halo formation or bloating of droplets using cellular automata.

A lattice consisting of 100 x100 square cells is considered for the study. The species under consideration are carbon (C), oxygen (O), carbon monoxide (CO) and iron (Fe). A sample distribution with states is shown in Fig. 4.

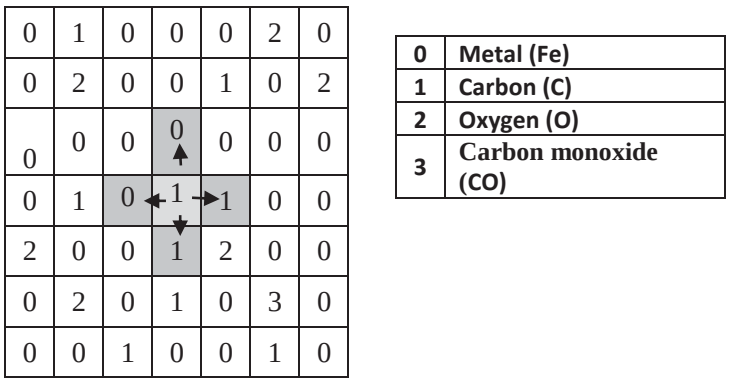

Figure 4. Newman Neighborhood with state number for the species considered for decarburization. Possible transition positions are shaded and arrows are depicting a possible exchange during diffusion.

Out of 100x100 grid, carbon is distributed in 98x98 grid leaving 2 rows of cells from boundaries. The two cells from the boundary are filled with oxygen such that the mole fraction of O is maintained. In the system, iron is considered as solvent. The initial distribution of C in the lattice is given on the basis of it concentration as mole fraction. The mole fraction of O is calculated from the equilibrium relationship denoted by Equation 1, where (%FeO) is the FeO concentration in the slag and [%O] is the oxygen concentration in the metal [34].

$$\frac{[\%O]}{(\%FeO)} = (0.1T - 155.3) \times 10^{-4} \quad (1)$$

Initially, CO presence is zero and the system is consisted with only of oxygen at the boundaries and carbon distributed throughout the 98x98 inner grid. The model can be divided into different subroutines, namely, diffusion, reaction and replenishment model. These subroutines are discussed in detail in the following sections.

3.1 Diffusion Model

Diffusion of species is calculated by random walk method. A species has the freedom to move in either of the cells in its Neumann neighbourhood. The possible events that can occur are i) the particle/species can move to any one cells among the four shaded cells (Newman neighborhoods) shown in Fig. 4 or ii) the particle may choose not to move at all. In the model under discussion, all these events are considered equi-probable and a random number is generated based on which one of the five events (movement in four directions and stationary state) are selected. The state of cells between which the movement occur are also get exchanged. The same process is repeated for oxygen but since the diffusivity of oxygen is two orders of magnitude higher than carbon, for one diffusion step of carbon, oxygen is allowed to diffuse 100 steps [35]. Also, in case of oxygen, the event for not moving is not considered, as under high concentration gradient and high diffusivity oxygen is highly probable to move. In this study, only carbon and oxygen are taken to be diffusing species however, exchange between CO and iron is not restricted. It is assumed that oxygen in the extreme boundary cells can 'jump' into the adjoining cells, if they are not blocked by CO.

3.2 Reaction Model

Once the diffusion subroutine is executed, the control is transferred to the reaction subroutine. The reaction rule is based on the state of neighbouring cells. The rule is defined as if the cell with state 1 (i.e. carbon) has a cell with state 2 (i.e. oxygen) in its Newman neighbourhood, then the reaction can occur and the state of cell is changed to 3 (i.e. carbon monoxide). Also, the cell with state 2, which participated in the reaction, is changed to 0 (denoting iron). If more than one cell with state 2 is present, one of them is randomly selected for the reaction. To summarize, one carbon cell reacts with one oxygen cell to form carbon monoxide. In the reaction subroutine, the lattice is divided into two zones A and B as shown in Fig.5. Zone A is around the boundary and is marked till 5 cells from the boundary while the remaining inner cells are in Zone B. It is assumed that carbon reacted in Zone A, and the formed CO here have a higher chance of contributing towards halo formation as it has a higher probability to escape into the boundary. On the contrary, carbon monoxide generated in Zone B has higher chance to contribute to bloating of the droplet as the bubbles formed here will have lower probability of escaping than Zone A bubbles. The demarcation is completely arbitrary due to absence of any validated study and difficulty in conducting the experiments to quantify the decarburization rate at different location in a droplet. The amount of carbon reacted in both the zones were recorded separately and stored for each time step.

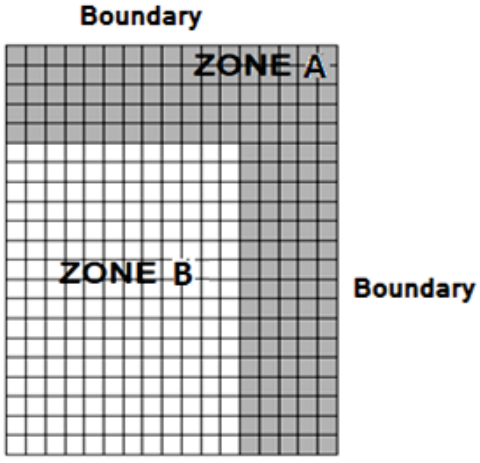

Figure 5. An upper right portion of grid under study depicting two zones with different rules

3.3 Replenishment Model

After the reaction step, as the oxygen is consumed, a count on oxygen consumption is maintained. As discussed earlier, the concentration of oxygen in metal is determined by the FeO in slag by equation 1. So, the used oxygen must be resupplied in order to keep the concentration constant. The consumed oxygen that have reacted, is resupplied by replacing the iron cells in second last boundary cells.

The model was run for 600 iterations with different oxygen potential and initial carbon content.

4. Results and Discussion

In the simulation, carbon and oxygen are allowed to diffuse and if the reaction condition as mentioned in section 3.2 is satisfied, the reaction is allowed to occur and carbon monoxide is generated. Here the initial carbon percentages (C_0) are taken as 3.8 wt. %, 1.7 wt. % and 0.8 wt. %. Similarly, different potentials of oxygen depending upon the % FeO in slag are taken. The FeO amount are taken as 10 wt. %, 20 wt. % and 30 wt. %. The plots of decarburization with varying initial carbon percentages are shown in Fig. 6 for 30 wt. % FeO. The effect of FeO content in the slag on decarburization curve is plotted in Fig. 7. The rate of decarburization decreased with decreasing FeO wt. % in slag. As discussed earlier, decarburization in Zone A and Zone B are calculated separately. Fig. 8 shows the percentage of decarburization occurred in Zone A (with respect to total carbon monoxide generated in both zones) for different initial carbon concentrations. Fig. 9 plots the same parameter with different FeO content in slag having 3.8 wt. % FeO content. In all the above simulations, we have defined Zone A till a distance of 5 boundary cells from the boundary. A simulation is then performed with this distance increased to 10 boundary cells in Zone A. The result for the same is shown in Fig. 10. A snapshot of lattice at 150th iteration of a simulation run is shown in Fig. 11. The background light green colour is of iron, the CO, carbon and oxygen is shown in yellow, light blue and dark blue respectively. *T*he simulation results are further discussed in the following sections.

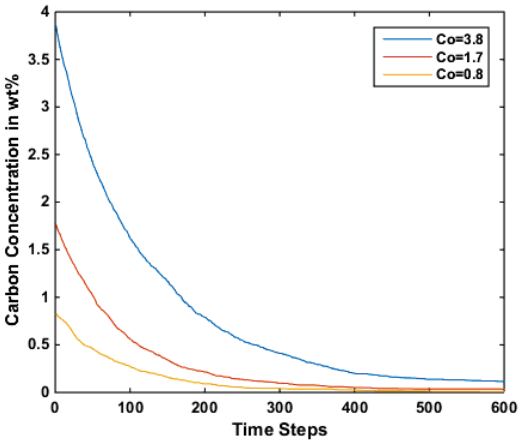

Figure 6. Decarburization with varying initial carbon concentration in droplet with 30 wt.% FeO in slag

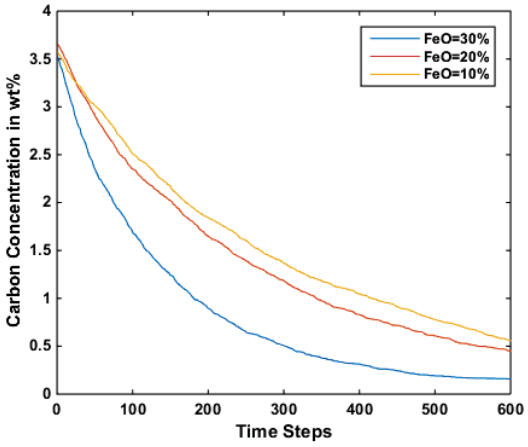

Figure 7. Decarburization of 3.8 wt.% carbon with varying FeO wt.% in slag

4.1 Effect of initial carbon concentration

In the study, higher decarburization rate is observed for systems with higher initial carbon contents, as shown in Fig. 6. In Fig. 8, the initial amount of carbon has a positive effect on the percentage of carbon monoxide formed in Zone A, when the oxygen potential is constant, though the increase of magnitude is not that large. This result is in agreement with the conclusion of Chen and Koley [13, 14]; according to their result, higher carbon content should favour halo formation i.e. higher percentage of carbon monoxide in Zone A. One of the reasons for the low increment can be attributed to the simplicity of the present model. As discussed above, the transport of species only inside the droplet is considered. The transport in slag and across the halo is not considered. Non-inclusion of this phenomenon may have increased the diffusion rate of oxygen resulting in faster diffusion of oxygen towards the centre in the model than in real phenomenon.

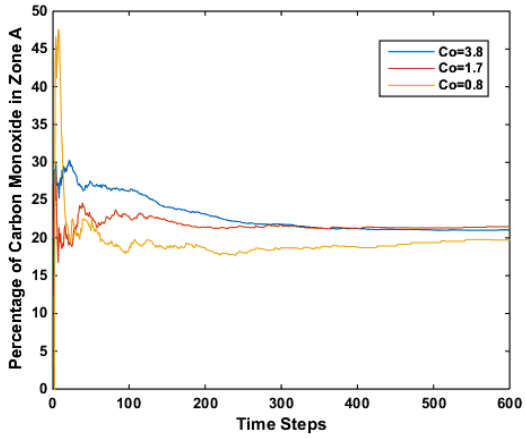

Figure 8. Percentage of CO in Zone A with varying initial carbon concentration

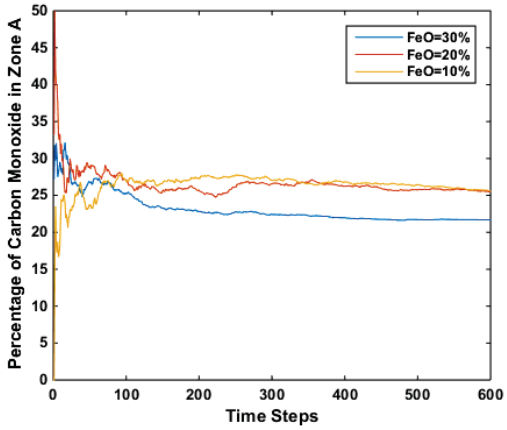

Figure 9. Percentage of CO in Zone A with varying slag FeO wt.% (C_0=3.8 wt.%)

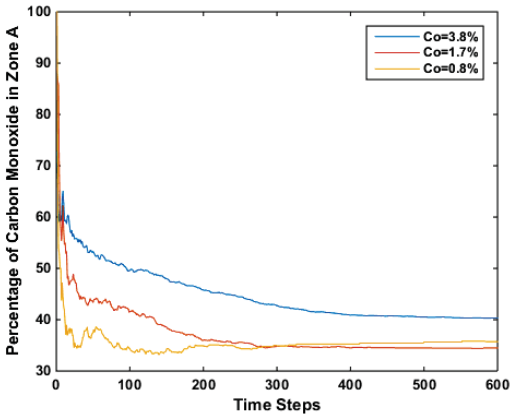

Figure 10. Percentage of CO in Zone A with varying initial carbon concentration and 10 cell zone A

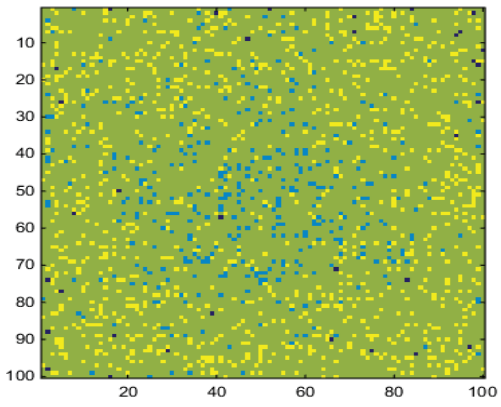

Figure 11. Intermidate state of a simulation, Co=3.8 wt.% FeO=30 wt.% at 150th time step

4.2 Effect of oxygen potential

The oxygen potential is defined as a function of FeO content in the slag using equation 1. In experimental studies by Gaye and Riboud [15], higher decarburization rate has been observed with increasing FeO content. Similar observation has been witnessed from the results of the present model. The Oxygen potential affected the decarburization rates and higher FeO wt.% in slag resulted in higher decarburization rates as shown in Fig.7. The effect on percentage of carbon monoxide in Zone A is shown in Fig. 9. The percentage of CO in zone A decreases with higher FeO in the slag; as with higher oxygen potential, higher amount of oxygen cells were present in the droplet. Due to high number of oxygen cells, more oxygen 'cells' were able to migrate towards the interior and react. In the case with varying carbon content, the difference in value is not considerable and the reason can be similarly attributed to the simplicity of the model and non-inclusion of transport in slag and across interface.

4.3 Effect of size of Zone A

Most of the above simulations (Fig. 6-9) are performed with size of Zone A limited to 5 boundary cells from the edge. In a simulation run, the Zone A boundary size is increased to 10 cells. As a result, the percentage of CO formed in Zone A increases as more cells come under it, as shown in Fig. 10.

Though, the values of percentage of CO in Zone A show some trends, but it is difficult to directly relate it to actual conditions as the selection of size of Zone A is completely arbitrary and it is also very difficult to validate. However, this can be one of the methods to demarcate the mechanisms of halo formation and bloating. Both of these mechanism involve formation of CO bubble but the behaviour of bubble is different. In gas halo mechanism, the bubble may easily escape forming a region between the slag and metal droplet whereas the bubble involved in bloating mechanism, may not escape and grow inside the droplet and may even cause bursting of droplet. However, the two parameters – the initial C concentration and the oxygen potential behave as reported in the earlier literature [13, 14]. The percentage of CO in Zone A can be studied in more detail when the model is augmented to include other phenomena like mass transfer kinetics across slag and gas halo, which are under development.

We have used cellular automata model successfully and highlighted how the complex behaviour of the decarburization process involving different phenomena can be simulated using simple local rules. In this model, the rules for diffusion and reaction are defined only locally to simulate the global complex behaviour. To understand the ease of implementation of rules, a case of limited oxygen mobility is simulated and the result is shown in Fig. 12. The result shows that if the diffusion or supply of oxygen inside the droplet is partially restricted, the reactions will happen mostly near the interface for a longer duration of time. The only change in this model is that the oxygen in the extreme boundary is not allowed to diffuse. This causes a drop in oxygen available for reaction in the central portion of the lattice, causing an increase in the percentage of carbon in Zone A.

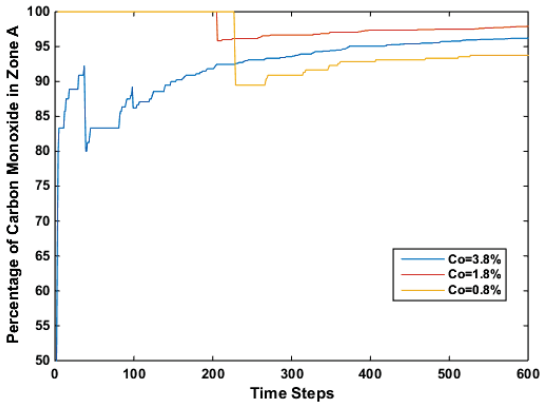

Figure 12. Percentage of CO in Zone A under restrictive supply of oxygen

The rules decided for the present model are unique in order to explain decarburization. The rules are open ended and are capable of incorporating further complexity to represent the actual phenomena occurring during steel making. Also, there can be more than one rules to simulate a certain phenomenon. For example, there are multiple ways to implement diffusion, like, using models by Chopard and Droz [29], or Weimar [30], as well as different rules for reactions as discussed by Kier et. al. [36]. The flexibility of making small changes at local level to reflect a complex global phenomena makes cellular automata a powerful tool to study complex processes like steelmaking as demonstrated in the present work. The authors expect that the current work may inspire other researchers to develop their own cellular automata rules for the decarburization and other complex phenomena in domain of process metallurgy.

5. Conclusions

In the present work, a cellular automata based model is developed to study decarburization in steelmaking process. The model is successful in capturing the effects of initial carbon concentration and FeO content of slag on decarburization. A study to evaluate the dominance of halo forming mechanism and bloating mechanism is also proposed based on the distance of formed CO from the boundary of the droplet. Further development of the model to include mass transfer in slag and across the gas halo is under progress.

References

[1] Ghosh A and Chatterjee A 2008 *Ironmaking and Steelmaking* (New Delhi: Prentice-Hall of India)
[2] Meyer H, Porter W, Smith G and Szekely J 1968 *Journal of Metals* **20** 35
[3] Kozakevitch P 1969 *Journal of Metals* **22** 57
[4] Dogan N, Brooks G and Rhamdhani M 2011 *ISIJ Int.* **51** 1086
[5] Dogan N, Brooks G and Rhamdhani M 2011 *ISIJ Int.* **51** 1093
[6] Dogan N, Brooks G and Rhamdhani M 2011 *ISIJ Int.* **51** 1102
[7] Urquhart R and Davenport W 1973 *Canadian Metallurgical Quarterly* **12** 507
[8] Millman M, Overbosch A, Kapilashrami A, Malmberg D and Bramming M 2013 *Transactions of the Indian Institute of Metals* **66** 525
[9] Mulholland E, Hazeldean G and Davis M 1973 *Journal of Iron and Steel Institute* **211** 632
[10] Molloseau C and Fruehan R 2002 *Metall and Materi Trans B*, **33** 335
[11] Sarkar R, Gupta P, Basu S, Ballal N B 2015 *Metall and Materi Trans B* **46** 961
[12] Brooks G, Pan Y, Subagyo and Coley K 2005 *Metall and Materi Trans B* **36** 525
[13] Chen E 2011 *Kinetic Study of Droplet Swelling In BOF Steelmaking*, PhD Thesis, McMaster University
[14] Chen E and Coley K 2010 *Ironmaking & Steelmaking* **37** 541
[15] Gaye H and Riboud P V 1977 *Metall and Materi Trans B* **8** 409
[16] Pan W, Sano M, Hirasawa M and Mori K 1991 *ISIJ Int.* **31** 358
[17] Sun H 2006 *ISIJ Int.* **46** 1560
[18] Von Neumann J and Burks A W 1966 *Theory of self-reproducing Automata (*Urbana: University of Illinois Press)
[19] Kari J 2005 *Theoretical Computer Science* **334** 3
[20] Batty M 2005 *Cities and Complexity (*Cambridge, Mass.: MIT Press)
[21] Kansal A, Torquato S, Harsh G, Chiocca E and Deisboeck T 2000 *Journal of Theoretical Biology* **203** 367
[22] Moreira J and Deutsch A 2002 *Advances in Complex Systems* **05** 247
[23] Wei Y, Ying S, Fan Y and Wang B 2003 *Physica A: Statistical Mechanics and its Applications* **325** 507
[24] Bartolozzi M and Thomas A 2004 *Physical Review E* **69** 046112
[25] Seybold P, Kier L and Cheng C 1997 *Journal of Chemical Information and Modeling* **37** 386

[26] Kier L, Cheng C, Tute M and Seybold P 1998 *Journal of Chemical Information and Modeling* **38** 271
[27] Neuforth A, Seybold P, Kier L and Cheng C 2000 *International Journal of Chemical Kinetics* **32** 529
[28] Parez-Terrazas J, Ibarra-Junquera V and Rosu H 2008 *Korean Journal of Chemical Engineering* **25** 461
[29] Chopard B and Droz M 1991 *Journal of Statistical Physics* **64** 859
[30] Weimar J 1997 *Parallel Computing* **23** 1699
[31] Adamatzky A, Martanez G and Mora J 2006 *International Journal of Bifurcation and Chaos* **16** 2985
[32] Van der Ween P, Baetens J and Baets B 2011 *J. Comput. Chem.* **32** 1952
[33] Toffoli T, Margolus N 1991 *Cellular Automata Machines* (Cambridge: MIT Press)
[34] Turkdogan E 2000 *ISIJ Int* **40** 964
[35] Kawakami M, Yokoyama S, Takagi K, Nishimura M and Kim J S 1997 *ISIJ Int.* **37** 425
[36] Kier L, Seybold P and Cheng C 2005 *Cellular Automata Modeling of Chemical Systems* (Netherlands: Springer).